Geoderma 438 (2023) 116633

Contents lists available at ScienceDirect

Geoderma

journal homepage: www.elsevier.com/locate/geoderma

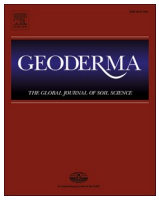

Hydrological characteristics and available water storage of typical karst soil in SW China under different soil–rock structures

Yanqiu Li [a,b,c], Shijie Wang [a], Tao Peng [a,c,*], Guozheng Zhao [a,c], Bin Dai [a,b,c]

[a] State Key Laboratory of Environment Geochemistry, Institute of Geochemistry, Chinese Academy of Sciences, Guiyang 550081, China
[b] University of Chinese Academy of Sciences, Beijing 100049, China
[c] Puding Karst Ecosystem Research Station, Chinese Academy of Sciences, Puding 562100, China

ARTICLE INFO

Handling Editor: L. Morgan Cristine

Keywords:
Soil hydrology characteristics
Karst
Plant available water
Land use
Soil–rock structures

ABSTRACT

Soil hydrological characteristics are influenced by factors such as parent rock weathering, human activities, and soil texture. However, the influence of the complex soil–rock structures and heterogeneous soil types on soil hydrological characteristics resulting from the weathering of carbonate rocks into soils on slopes in the karst region of SW China is not fully understood. The relationships between zonal and nonzonal soil hydrological characteristic differences, land uses, and soil–rock structures were analyzed using a typical watershed in the SW China karst region. In this study, (1) the difference between zonal and nonzonal soil hydrological characteristics is significant. For infiltration capacity (K_s), yellow soil (19.50 ~ 1058.00 cm·d^{-1}) < limestone soil (34.50 ~ 2364.00 cm·d^{-1}), while for soil available water storage, limestone soil on the dolomitic slope (43.26 mm) > yellow soil (20.16 ~ 35.25 mm) > limestone soil on the limestone slope (17.73 ~ 34.72 mm). (2) Land-use practices and soil–rock structures have long affected the hydrological characteristics of soil in karst. (3) The bare bedrock on carbonate slopes leads to a reduction in the total amount of soil per unit area on the slope, which compresses the space for vegetation growth and reduces the total amount of water provided by the soil for vegetation growth per unit area, which confirms one of the reasons for the low plant biomass in karst. These results suggest that the utilization of soil water in karst areas should consider the weights of soil type, lithology, and soil–rock structures.

1. Introduction

As the junction of the atmosphere, lithosphere, hydrosphere, and biosphere, the soil is an important component of the Earth's system and plays an important role in climate regulation and the water cycle (Ouyang, 2002; Ford and Williams, 2007; Mujica and Bea, 2020). As healthy soil provides plant growth and development and inhibits the occurrence of soil erosion on slopes, it is important to clarify the soil hydrological characteristics for various reasons, such as agricultural production, vegetation restoration and environmental protection. A large body of literature has shown that soil hydrological characteristics such as water infiltration, vegetation water use, and evaporation are influenced by vegetation restoration, land use, topography/geomorphologic background, soil texture and so on (Kramer, 1969; Jonsson et al., 2004; Chen et al., 2009; Zhao et al., 2014; Fu et al., 2016). However, in addition to vegetation restoration, land use, topography/landscape and soil texture, the soil hydrological characteristics and the available water content in karst areas with complex soil–rock structures and multiple soil types have not been reported (Zhang et al., 2014; Fu et al., 2016; Liu et al., 2019; Mujica and Bea, 2020; Zhong et al., 2022).

Karst landforms, which are one of the major natural landscapes in the world, occupy 20% of the global land surface (Ford and Williams, 2007; Wang et al., 2019b). In China, karst landscapes are mainly distributed in the southwestern regions. In recent decades, the process of soil degradation caused by increasing population and irrational land use has mainly manifested by the reduction of vegetation cover, severe soil erosion, extensive exposed carbonate rocks, drastic declines in the productivity of the agricultural industry and water–holding capacity, fragile ecological functions, and the emergence of a desertification–like landscape (Wang et al., 2004; Cao et al., 2008; Peng and Wang, 2012; Peng et al., 2019a; Wang et al., 2019b). After years of ecosystem restoration programs, the state of vegetation restoration in karst areas of China is excellent (Tong et al., 2013; Yang et al., 2017). Most of the current reports related to soil hydrological characteristics have focused

* Corresponding author at: State Key Laboratory of Environment Geochemistry, Institute of Geochemistry, Chinese Academy of Sciences, Guiyang 550081, China.
E-mail address: pengtao@mail.gyig.ac.cn (T. Peng).

https://doi.org/10.1016/j.geoderma.2023.116633
Received 4 August 2022; Received in revised form 26 May 2023; Accepted 3 August 2023
Available online 21 August 2023
0016-7061/© 2023 Published by Elsevier B.V. This is an open access article under the CC BY-NC-ND license (http://creativecommons.org/licenses/by-nc-nd/4.0/).

on the effects of vegetation restoration, human activities, topography/landscape, and soil texture (Chen et al., 2009; Zhao et al., 2014; Peng et al., 2019b). However, in addition to these influencing factors, the complex soil–rock structures caused by the phenomenon of exposed bedrock, which is unique to karst areas, have a significant impact on the total amount of soil on slopes. Scholars conclude that the relationship between soil–rock structures and land use is obvious, as slopes with more exposed bedrock have less total soil and are mostly secondary forests, while the foot of the slope has less bare bedrock and richer soil for agricultural activities (Zhang et al., 2012; Zhong et al., 2022). Such differential soil–rock structures result in highly inhomogeneous karst soils, and the water infiltration capacity is much higher than that of nonkarst areas. The existence of dominant flow at the rock–soil interface results in rapid soil hydrological processes on the surface of karst slopes (Sohrt et al., 2014; Fu et al., 2016; Yang et al., 2016; Peng et al., 2019b; Wang et al., 2019a). The differences in saturated hydraulic conductivity and soil water retention curves in the results of scholars' research are influenced by soil properties and complex topographic conditions and land use, which also confirm this phenomenon (Wang et al., 2015; Liu et al., 2021). Similarly, the staggered distribution of exposed rocks and soil alters local hydrological processes, with bare rocks pooling water into the soil and increasing soil water content (Sohrt et al., 2014; Wang et al., 2016). Additionally, in the underground fissure network formed by carbonate rocks, there is an important channel in which water and soil resources can leak downward, which makes water and soil erosion not only appear on the surface but also underground leakage; these conditions result in low total soil and low water storage capacity on karst slopes, and extremely low surface runoff coefficients, ultimately causing water shortages in the region (Peng and Wang, 2012; Fu et al., 2015; Liu et al., 2019; Peng et al., 2019a). Differences in lithology also produce differential soil–rock structures, with continuous but shallow soil on dolomite slopes and deeper soil on limestone slopes with fissure development, which affect their soil hydrological processes (Liu et al., 2019; Chen et al., 2022; Zhong et al., 2022).

In addition to the above influencing factors, soil types in karst areas are not uniform. Zonal soil and nonzonal soil are interlaced, which greatly influences the soil structure in this region and causes differences in soil hydraulic characteristics (Cao et al., 2008; Bai and Zhou, 2020). Limestone soil and zonal yellow soil are the typical soil types in karst areas of Southwest China (following Chinese soil classification) (Cao et al., 2003). The parent material of limestone soil is carbonate rock. In the warm and humid subtropical climate, the initial limestone soil weathered from carbonate rock is usually located in the higher parts of the landscape, while the limestone soil that has undergone the process of decalcification by rainwater leaching is enriched into yellow limestone soil at the foot of slopes and in depressions where the landscape is relatively low. This kind of soil mostly appears in the peak–cluster depression in the upper watershed. Zonal soil (yellow soil) can be found at the later stage of weathering from carbonate rock into soil or can be weathered from sandstone, shale, basalt, and clayey old weathering crust. In karst areas, this kind of soil is distributed in the relatively flat peak forest plain (Davey et al., 1975; Cao et al., 2003; Zhang et al., 2014; Bai and Zhou, 2020). The limestone soil on carbonate slopes is shallow and fragmented, and plant roots tend to grow more laterally than vertically, with 89% of the roots distributed in the 0–20 cm soil layer, while the biomass of mixed evergreen broadleaf forests in the region is lower than that of nonkarst forests in subtropical China (Nie et al., 2014; Ni et al., 2015). In contrast, the yellow soil distributed in the peak forest plains is deep, but the plant roots are mostly concentrated in the 0 ~ 30 cm soil layer (more than 82%), and the biomass is also higher than that of the limestone soil (Han et al., 2017).

In summary, most studies on the soil hydrological characteristics of karst slopes have focused on the pooling of water by exposed carbonate rocks and slope hydrological processes, but there has been no in–depth study on the effect of soil–rock structures on soil hydrological characteristics, and the available water storage capacity of slopes with different soil–rock structures has not been quantified. These factors affect the stability of the ecosystem and the sustainable development of agriculture, as well as the configuration of the landscape pattern and the configuration of hydraulic facilities. To compare and analyze the hydraulic properties and ecohydrological effects of typical karst soils (limestone soil, yellow limestone soil and yellow soil) in a typical karst watershed (Houzhai watershed, which is located in Puding County, central Guizhou Province, Southwest China) of Southwest China, their geological background and soil–rock structures were selected and combined. Representative soil indices, such as soil bulk, saturated water conductivity and soil water characteristic curves, were selected for measurement. The main objectives were to (1) determine the differences between zonal soil and nonzonal soil hydrological characteristics; (2) determine the influences of land-use change and soil–rock structure on soil hydrological characteristics; and (3) evaluate their water supplying capacities and influencing factors. The results of this study can provide a reliable scientific basis for future water resource allocation and agricultural industry layout in karst ecosystems.

2. Materials and methods

2.1. Study region

The samples were collected in the Houzhai watershed (105°40′43″–105°48′2″E, 26°12′29″–26°17′15″N), which covers an area of 72 km^2 and is located in Puding County in the central part of Guizhou Province in Southwest China. The watershed has a subtropical monsoon climate with high humidity. The annual mean temperature is 15.6 °C. The soil types in this county are mainly limestone soil and yellow soil, which together account for more than 80% of the soil area of the county and are representative of Southwest China (Zhang et al., 2021). The watershed of the basin is high in the southeast and low in the northwest, with an average altitude of 1300 m, a maximum elevation of 1585 m and a minimum elevation of 1018 m, and the relative height difference is generally 250 ~ 300 m. The watershed of the basin is undulating, and the geomorphological trend from upstream to downstream is peak depression, peak forest basin and hill valley. The slope of the peak depression is a shallow black limestone soil formed by the weathering of carbonate rock, and the vegetation is secondary forest after reforestation (the main vegetation consists of *Pyacantha fortuneana*, *Platycarya longipes*, *Rosa cymosa*, etc.), while the yellow limestone soil in the depression at the foot of the slope is formed by the leaching of the black limestone soil after washing and accumulating on the slope. Local farmers carry out their agricultural activities mostly on yellow limestone soil with a thick soil depth at the foot of the slope. In the peak forest basin, the gradient of the slope changes gently; a small amount of the steeper slope is black limestone soil vegetation that is mostly secondary trees and shrubs (the dominant vegetation is similar to that on the black limestone soil of the slope in the peak depression), while the gentle slope is yellow limestone soil, used mostly for agriculture. Yellow soil with a zonal distribution starts to appear and is mostly used as agricultural land by local residents, and the natural vegetation is mostly *Cunninghamia lanceolata* and *Pinus massoniana*, which are suitable for growth in acidic soil. In the hill valley, the soil was mainly deep yellow soil with a zonal distribution, the limestone soil is scattered on some slopes, and the yellow soil area is similar to the peak forest basin, which is used for agriculture and has vegetation, such as *C. lanceolata*, *P. massoniana* and other vegetation (Liu et al., 2016; Zhang et al., 2021).

2.2. Sample design

In this study, six soil profiles were collected in the Houzhai watershed (Table 1 and Fig. 1). They included dolomite slope grassland (DG), limestone slope shrub (LS), limestone slope abandoned farmland (LA), yellow limestone soil tillage (YLT), yellow soil tillage fruit forest (YFT), and yellow soil forestland (YF). The DG sample site was collected from

Table 1
Summary of characteristics of soil samples.

Filds	Position	Slope (°)	Stone (%)	Land use	Dominant plant species
DG	Middle	38	15	Grazing (2007) Grazing (2020)	*Themeda japonica* and *Heteropogon contortus*
LS	Middle	33	50	Grazing (2007) Shrub(2020)	*Pyacantha fortuneana, Coriaria nepalensis, Rosa cymosa*
LA	Middle	37	40	Farmland (2007) Trees and shrubs(2020)	*Platycarya longipes* and *Itea yunnanensis*
YLT	Foot	18	10	Farmland (2007) Farmland (2020)	*Corn* and *oilseed rape*
YFT	Foot	11	0	Farmland (2007) Farmland (2020)	Fruit tree
YF	Foot	9	0	Forests (2007) Forests (2020)	*Cunninghamia lanceolata* and *Pinus massoniana*

black limestone soil formed by weathering on dolomite slopes. The area was covered with shrubs and grass the same year and grazed by local farmers year-round. The soil thickness was within 10 cm, and the slope position was located on the upper slope. The LS sample site had black limestone soil, and the sample site was used by local farmers for grazing until 2007. After that, the Chinese government implemented the "Grain for Green" project, and the sample site was gradually converted to scrubland after natural restoration. The soil thickness was approximately 30 cm, and the samples were collected from the middle of the slope. The LA sample site had black limestone soil. It was used by local farmers for farming, and the sample site had severe soil erosion leading to land degradation, which posed a great threat to the local ecological environment after the fire in 2007. The sample site included a tree and shrubs after natural recovery. The soil thickness was 30 cm, and the sample was collected from the middle of the slope. The YLT sampling site was at the foot of the limestone slope, which belonged to the yellow limestone soil formed by leaching after deposition at the foot of the slope. The sample site has long been planted by local farmers with cash crops such as corn. The soil layer was relatively deep, up to 30 ~ 100 cm. The YFT sample site had a zonally distributed yellow soil, which had been used as agricultural land for cultivation for many years with high human disturbance, and during the study period, the local farmers planted peach trees as a cash crop. The soil depth was greater than 1 m. The YF sample site had a zonally distributed yellow soil, and its vegetation was *C. lanceolata* and *P. massoniana*, which can grow in acidic soil. The soil layer was very deep, greater than 1 m.

Due to the different soil depths in the karst slope, we considered collecting 0 ~ 30 cm soil for this study. For the dolomite slope sample site (DG), the soil depth was within 10 cm, and we collected only 0 ~ 10 cm soil. Before each sampling, surface litter and leaves were removed, and then soil profile samples were obtained from 0 ~ 10, 10 ~ 20, and 20 ~ 30 cm of the soil pit wall. Three cutting rings (250 cm^3) were used for each layer of soil to collect soil samples, after which the samples were brought back to the laboratory for determination and analysis. If the soil depth was too shallow, i.e., <30 cm, the samples were collected to bedrock.

2.3. Lab analysis

First, the measurement of capillary porosity (CP, %), noncapillary porosity (NCP, %), and soil bulk density (BD, g·cm^{-3}) of the undisturbed soil samples was described by (Fu et al., 2016; Yang et al., 2016). Second, K_s was measured with the KSAT® device based on the falling–head method and by using Darcy's equation (Reynolds and Elrick, 1990; Reynolds et al., 2000; Bagarello et al., 2012). The water retention curves were determined using the commercial device HYPROP® to conduct the evaporation method (Schelle et al., 2010; Schelle et al., 2013). Before the experiment, the soil cores were sealed at the bottom, placed on a scale and exposed to evaporation. The soil samples were continuously monitored by two tensiometers at depths of 1.25 and 3.75 cm, and the sample quality was recorded. The measuring range of the HYPROP® device was 0 ~ 3 pF. When pF > 3, we chose the WP4C PoteneiaMeter® to experiment with the dew point method (Schelle et al., 2013). After using the HYPROP® device, the soil samples were oven–dried at 105 °C for 48 h to determine the soil bulk density (BD).

Disturbed samples were used to determine particle size distribution using the hydrometer method (Yang et al., 2016). Soil organic carbon (SOC) was determined using an organic elemental analyzer (vario MACRO cube) produced by Elementar, Germany.

2.4. Data analysis

Statistical analyses were conducted using SPSS 22.0 for Windows. One–way ANOVA was used to analyze the means. The LSD test was used to compare the means of soil variables when the ANOVA results were significant among different vegetation types at the $p < 0.05$ level. Water retention curve data were fitted in the HYPROP FIT software by Van Genuchten (Schelle et al., 2010; Schelle et al., 2013), which was expressed as follows:

$$\theta(h) = \theta_r + \frac{\theta_s - \theta_r}{[1 + |\alpha h|^n]^m} \quad (1)$$

where $m = 1–1/n$ for $n > 1$; h is the soil water pressure head (cm), θ is the volumetric soil water content (mm), θ_r is the residual soil water content (mm), θ_s is the saturated soil water content (mm), and α (cm^{-1}) and n (dimensionless) are the fitting parameters in the soil water retention function. The reciprocal of α, $1/\alpha$ (cm), refers to the air entry value. To quantify the average discrepancy between the measured and model-predicted variables, the root mean square error (RMSE) was calculated for each data group contained in the objective function:

$$RMSE = \sqrt{\frac{1}{n_j}\sum_{i=1}^{n_j}\left[r_{ij}(p)\right]^2} \quad (2)$$

The water retention curve of a particular soil describes the relationship between the volumetric water content θ (mm) and matric head h (cm). The latter varies on a logarithmic scale and is therefore often expressed as a dimensionless pF value (pF = log10(−h)). Volumetric water contents (mm) at field capacity (FC = 2.5 pF) and permanent wilting point (PWP = 4.2 pF) were calculated. The available water content (AWC) was calculated by subtracting the water content at PWP from that at FC (Schelle et al., 2013). All figures were produced using Origin 9.1.

$$AWC = FC - PWP \quad (3)$$

3. Results

3.1. Variation in soil properties

The basic soil properties of this study are shown in Table 2. The pH of limestone soil ranged from 6.7 to 7.3, which was higher than the pH values of 4.9 to 5.0 in yellow soils. The soil bulk density of limestone soil ranged from 0.91 to 1.26 g·cm^{-3} and that of yellow soil ranged from 1.05 to 1.25 g·cm^{-3}. Except for the higher soil bulk density (1.26 g·cm^{-3}) at the LS and YLT sample sites from 0 to 10 cm in the limestone sample sites, the other sample sites showed an increasing trend with the

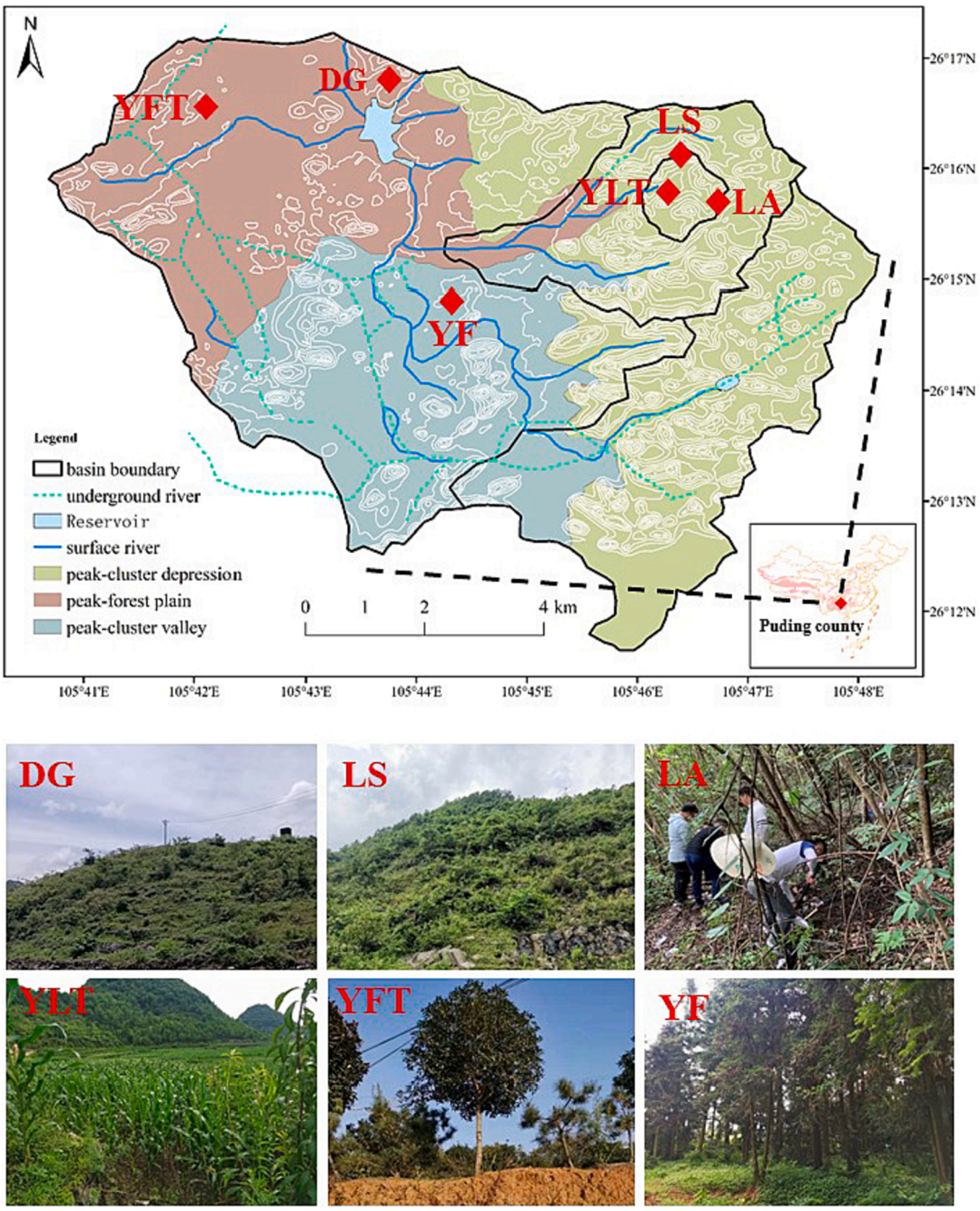

Fig. 1. Map of the study area. DG means dolomite slope grassland; LS means limestone slope shrub; LA means limestone slope abandoned farmland; YLT means yellow limestone soil tillage; YFT means yellow soil tillage fruit forest; YF means yellow soil forestland.

deepening of the soil layer, while the soil bulk density below 10 cm in the yellow soil sample sites was higher than that in the four limestone soil sample sites. The trend of soil organic carbon content was the opposite of the trend of bulk density, decreasing with the deepening of the soil layer; moreover, the highest organic carbon content (77.27 $g{\cdot}kg^{-1}$) was in the 0 ~ 10 cm soil layer of the LA sample site and the lowest organic carbon content was in the yellow soil sample site YFT. In addition, the organic carbon content of each soil layer in the four limestone soil sites was higher than that of the corresponding soil layer in the yellow soil sites. Except for LA, where CP decreased and NCP increased in the 10 ~ 20 cm soil layer, CP increased and NCP decreased with the deepening of the soil layer at all sample sites. In the limestone soil samples, the sand decreased with the deepening of the soil layer, while the silt particles and clay showed the opposite trend and increased. However, in the YFT and YF, only silt showed an increasing trend with soil depth, while sand and clay showed a decreasing trend.

3.2. Variation in K_s

As shown in Fig. 2, along with the deepening of the soil layer, all six sample plots selected for this study showed a decreasing trend of K_s. However, there were some differences among the different sites. For the nonzonal limestone soil sites, the mean K_s values ranged from 57.67 to 2364.00 $cm{\cdot}d^{-1}$ for the 0 ~ 10 cm soil layer, 34.50 to 1077 $cm{\cdot}d^{-1}$ for the 10 ~ 20 cm soil layer, and 35.00 to 829.00 $cm{\cdot}d^{-1}$ for the 20 ~ 30 cm soil layer. In contrast, in the zonally distributed yellow soil sample sites, the K_s ranged from 426.01 to 1058.00 $cm{\cdot}d^{-1}$ for the 0 ~ 10 cm soil layer, 19.50 to 55.50 $cm{\cdot}d^{-1}$ for the 10 ~ 20 cm soil layer, and 28.50 to 38.71

Table 2
Basic soil properties.

Name	Depth (cm)	pH	BD ($g \cdot cm^{-3}$)	SOC ($g \cdot kg^{-1}$)	CP (%)	NCP (%)	Sand (%)	Silt (%)	Clay (%)
DG	0 ~ 10	7.10 ± 0.08	0.91 ± 0.15	68.00 ± 5.71	54.20 ± 4.97	9.70 ± 5.73	21.54 ± 3.50	48.61 ± 4.93	29.85 ± 2.33
	0 ~ 10	7.02 ± 0.09	1.26 ± 0.13	56.74 ± 6.08	38.97 ± 7.01	16.40 ± 8.33	43.21 ± 3.46	35.98 ± 5.67	20.81 ± 4.18
LS	10 ~ 20	7.23 ± 0.07	1.19 ± 0.04	21.57 ± 3.22	41.80 ± 5.37	13.73 ± 7.50	32.15 ± 2.77	41.56 ± 3.04	26.29 ± 2.26
	20 ~ 30	7.12 ± 0.11	1.24 ± 0.07	18.75 ± 4.50	37.87 ± 3.85	10.23 ± 4.18	39.12 ± 4.13	42.21 ± 4.85	18.67 ± 1.24
	0 ~ 10	6.91 ± 0.05	0.97 ± 0.10	77.27 ± 8.88	47.80 ± 5.50	15.47 ± 3.13	28.36 ± 2.76	46.53 ± 3.04	25.11 ± 2.36
LA	10 ~ 20	7.14 ± 0.08	1.04 ± 0.12	44.54 ± 6.51	43.46 ± 6.37	21.70 ± 8.73	26.25 ± 3.09	48.56 ± 2.95	25.19 ± 3.22
	20 ~ 30	7.35 ± 0.10	1.12 ± 0.05	48.64 ± 5.99	44.87 ± 3.74	16.40 ± 6.27	21.56 ± 1.79	41.12 ± 4.85	37.32 ± 4.21
	0 ~ 10	6.73 ± 0.07	1.26 ± 0.12	20.58 ± 4.23	40.97 ± 6.33	16.40 ± 7.36	29.45 ± 2.84	42.82 ± 3.63	27.73 ± 2.38
YLT	10 ~ 20	6.92 ± 0.12	1.19 ± 0.15	19.42 ± 5.66	41.80 ± 4.71	10.73 ± 5.26	27.53 ± 3.82	43.17 ± 2.74	29.30 ± 3.85
	20 ~ 30	6.91 ± 0.03	1.22 ± 0.06	17.73 ± 6.93	41.87 ± 4.02	7.23 ± 3.77	22.12 ± 2.90	44.75 ± 4.03	33.13 ± 4.60
	0 ~ 10	4.92 ± 0.07	1.05 ± 0.11	19.08 ± 4.33	41.07 ± 4.33	17.40 ± 6.52	23.48 ± 3.71	46.31 ± 1.94	30.21 ± 4.27
YFT	10 ~ 20	4.98 ± 0.05	1.13 ± 0.08	14.70 ± 3.41	42.47 ± 3.77	13.47 ± 3.95	26.75 ± 2.74	48.91 ± 3.92	24.34 ± 4.10
	20 ~ 30	5.06 ± 0.04	1.25 ± 0.06	14.72 ± 2.97	48.63 ± 3.81	12.83 ± 5.51	21.22 ± 1.93	56.11 ± 4.93	22.67 ± 3.26
	0 ~ 10	4.74 ± 0.11	1.15 ± 0.11	36.30 ± 4.58	34.40 ± 3.01	20.87 ± 5.58	42.13 ± 2.87	32.15 ± 3.48	25.72 ± 2.42
YF	10 ~ 20	5.03 ± 0.05	1.12 ± 0.07	15.08 ± 3.86	41.70 ± 2.72	16.80 ± 5.88	31.26 ± 3.84	48.72 ± 2.38	20.02 ± 4.22
	20 ~ 30	4.94 ± 0.09	1.18 ± 0.09	15.29 ± 4.31	43.53 ± 2.59	11.37 ± 3.79	35.65 ± 4.27	44.76 ± 4.22	19.68 ± 3.50

DG means dolomite slope grassland; LS means limestone slope shrub; LA means limestone slope abandoned farmland; YLT means yellow limestone soil tillage; YFT means yellow soil tillage fruit forest; YF means yellow soil forestland; BD means soil bulk density; SOC means soil organic carbon; CP means soil capillary porosity; NCP means soil no-capillary porosity; Sand means soil sand content; Silt means soil silt content; Clay means soil clay content; pH means soil pH.

for the 20 ~ 30 cm soil layer. All the 30-cm limestone soils sampled and designed in this study had a stronger infiltration capacity than that of the yellow soil sites, while when the depth of the soil layer was deeper than 10 cm, the K_s of yellow soil sites had a more obvious decreasing trend and a lower infiltration capacity than the limestone soils.

3.3. Characteristics of the soil water retention curve and water–supply capacity analysis

As shown in Table 3, the van Genuchten function fitted the water retention curves of all study sites very well, with an RMSE below 0.09. The difference in soil texture among the six sample sites led to the different α values, but except for the LA and LYT samples, the α values of the fitted parameters for the surface soil were the largest of all the sample sites, indicating that the surface soil had lower air entry values and more noncapillary air.

Overall, the soil water retention curves all had high volumetric water content, indicating a good water holding capacity. There was a rapid decrease in the pF values from 0 to 2.5 for limestone soil, while the soil water retention curves of yellow soil samples had a decreasing trend only at a pF of 2.5, which indicated that although the saturated water content of limestone soil was higher, the ability of yellow soil samples to retain water was higher than that of limestone soil samples. The change in soil water retention curves in the surface layer decreased relatively rapidly with pF, while the trend of the soil water retention curves was relatively similar among all layers in the sample plots except for the LS

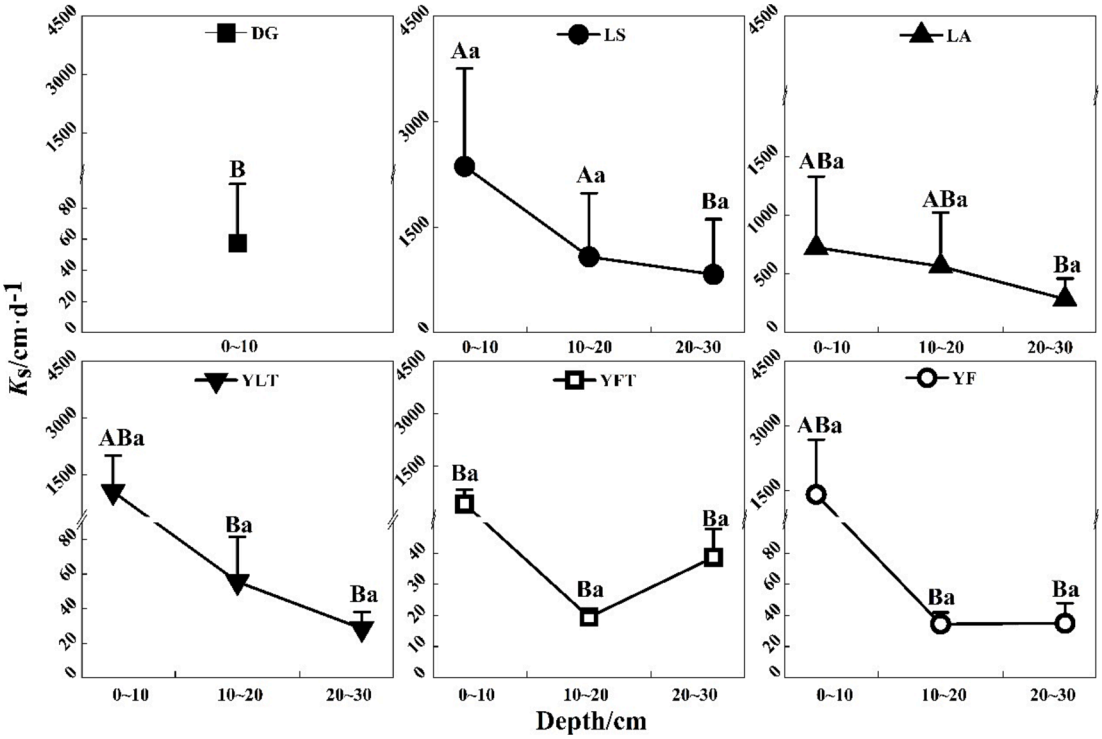

Fig. 2. Variations in saturated hydraulic conductivity (K_S) in the six samples. Different lowercase letters indicate significant differences with soil depth ($p < 0.05$), and different uppercase letters indicate significant differences in soil profiles at the same depth ($p < 0.05$).

Table 3
Fitting parameters of the van Genuchten equation.

Name	Soil Depth/cm	Parameters a (cm^{-1})	n	θ_s (mm)	θ_r (mm)	RMSE
DG	0 ~ 10	0.00190	1.523	0.611	0.004	0.0328
LS	0 ~ 10	0.07580	1.154	0.644	0.008	0.0035
	10 ~ 20	0.00300	1.245	0.487	0.004	0.0526
	20 ~ 30	0.00600	1.134	0.694	0.005	0.038
LA	0 ~ 10	0.00320	1.327	0.615	0.004	0.0305
	10 ~ 20	0.016100	1.177	0.064	0.001	0.0426
	20 ~ 30	0.007250	1.171	0.589	0.003	0.0807
LYT	0 ~ 10	0.004070	1.277	0.582	0.027	0.0459
	10 ~ 20	0.004920	1.198	0.492	0.025	0.0331
	20 ~ 30	0.004480	1.333	0.428	0.025	0.0536
YFT	0 ~ 10	0.002860	1.238	0.565	0.024	0.0533
	10 ~ 20	0.00240	1.291	0.565	0.022	0.0531
	20 ~ 30	0.00122	1.409	0.552	0.002	0.0245
YF	0 ~ 10	0.06460	1.184	1.325	0.039	0.0811
	10 ~ 20	0.00203	1.300	0.554	0.040	0.0297
	20 ~ 30	0.02010	1.025	0.637	0.034	0.0144

DG means dolomite slope grassland; LS means limestone slope shrub; LA means limestone slope abandoned farmland; YLT means yellow limestone soil tillage; YFT means yellow soil tillage fruit forest; YF means yellow soil forestland.

and YF sample plots (Fig. 3).

As shown in Table 4, the available water content (AWC) of the four limestone sample sites in this study ranged from 17.73 mm to 43.26 mm. In addition, the AWC of the limestone samples was lower than that of the yellow soil samples at 10 ~ 30 cm, ranging from 20.95 to 23.41 mm, while that of the yellow soil samples tended to increase with the deepening of the soil layer, with values ranging from 24.16 to 35.25 mm. In conclusion, the surface limestone soil had a better effective water content than the yellow soil below 10 cm and could better provide water for plants.

3.4. Correlation analysis between Ks, FC, PWP, AWC and influencing soil properties

The results of the Pearson correlation analysis between each soil property, *Ks* and AWC are shown in Table 5. K_s was extremely significantly correlated ($p < 0.01$) with sand content and silt content and significantly correlated with CP ($p < 0.05$). AWC was extremely significantly correlated with CP and silt content and significantly correlated with BD and sand content. The available water content and infiltration capacity of the soil were mainly influenced by the soil texture.

4. Discussion

4.1. The difference in soil hydrological characteristics between nonzonal and zonal soil

There were obvious differences in BD, SOC, K_s, etc., between limestone soil and yellow soil The reason was that the difference in soil parent material produced differences in soil type and soil –rock structure, which in turn affect the internal physical structure and chemical properties of the soil (Zhao et al., 2014; Yang et al., 2016; Cardelli et al., 2017). Limestone soil, which was widely distributed on slopes and formed by limestone weathering, had a higher permeability than yellow soil, which was closely related to soil texture through correlation analysis (Table 4). The limestone soil showed a decrease in sand content and an increase in clay content with the deepening of the soil layer, showing an increasingly viscous phenomenon, while the yellow soil showed an increasingly enriched silt content with the deepening of the soil layer. Soil texture affected the infiltration capacity, similar to the results of Chen et al. (2012), who reported that sand content promoted soil infiltration capacity in karst areas, and Chen also believed that the abundance of rock fragments in karst slopes affected the infiltration capacity

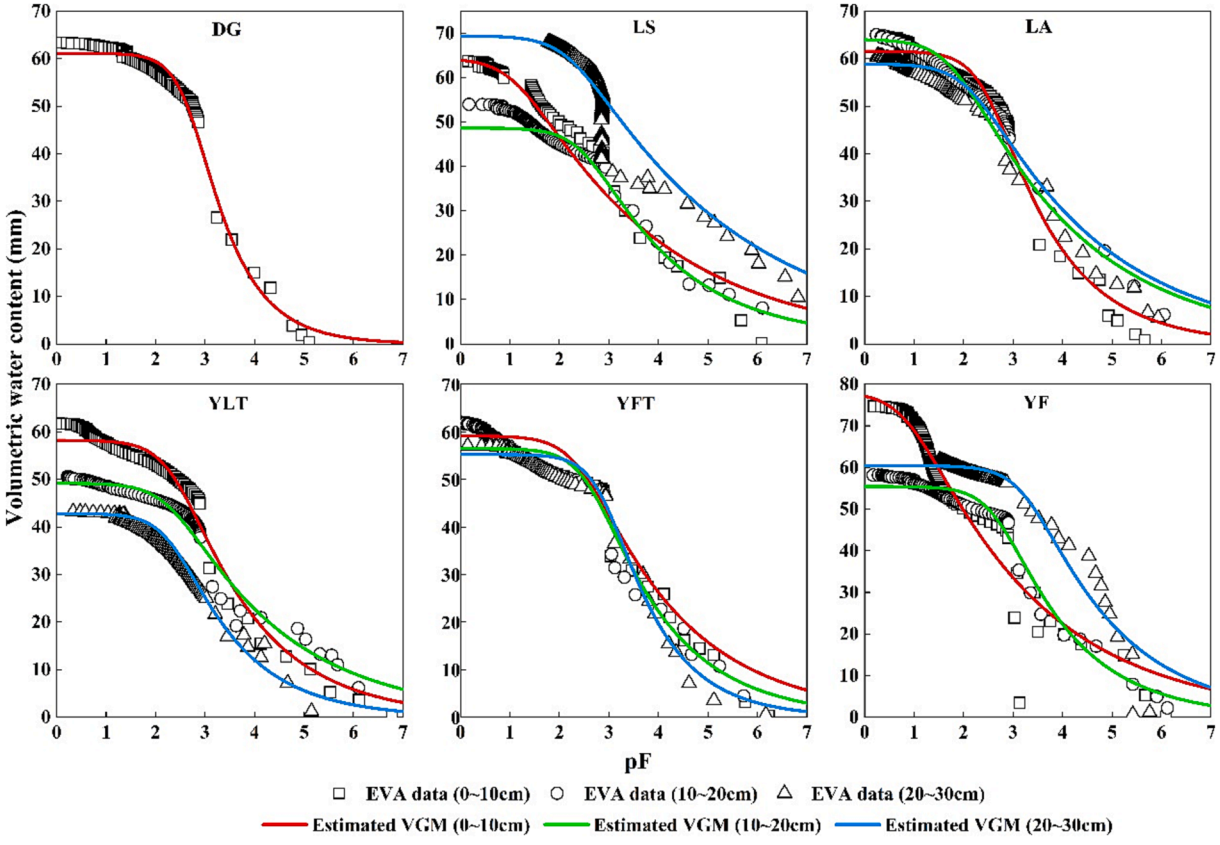

Fig. 3. Vertical characteristics of water retention curves. EVA data means water retention data obtained with the evaporation (eva) method by HYPROP® and WP4C PoteneiaMeter®; VGM means the van Genuchten model; pF means the dimensionless pF value (pF = log10(−*h*)).

Table 4
Vertical variations in available water content (mm).

	DG	LS	LA	YLT	YFT	YF
0 ~ 10	43.26	17.73	34.72	29.87	27.30	20.16
10 ~ 20		23.39	23.04	20.95	27.23	30.51
20 ~ 30		23.06	22.64	23.41	35.25	24.16

DG means dolomite slope grassland; LS means limestone slope shrub; LA means limestone slope abandoned farmland; YLT means yellow limestone soil tillage; YFT means yellow soil tillage fruit forest; YF means yellow soil forestland.

of soil in this area. The difference in soil texture also caused the difference in water supply capacity, and related reports indicated that sand content inhibited soil AWC and silt content promoted it (Salter and Williams, 1965).

In this study, the surface layer (0 ~ 10 cm) of limestone soil had more silt content and thus had more available water content than the yellow soil (Table 2), but as the soil layer deepened, the sand content of limestone soil decreased and the clay content increased, resulting in a more sticky soil, while the silt content of yellow soil increased with the increase in the soil layer and, thus, increased the available water content (AWC), indicating that the 10 ~ 30 cm layer of yellow soil provided more water for vegetation development. The soil layer of 30 cm could provide more available water for vegetation growth and development, so local agricultural activities were mostly carried out in the area where the topography was flat and yellow soil was distributed. During the formation of limestone soils, the parent rock (carbonate rock) was enriched in calcium (Ca) and magnesium (Mg) elements, which led to high alkaline soil pH. Additionally, the enriched calcium ions in limestone soil could form organic complexes with organic carbon to preserve organic carbon or organic carbon that was encapsulated in secondary carbonate rock, which made limestone soil have a high organic carbon content (Zhu et al., 2016; Wang et al., 2018; Di et al., 2019).

Dolomite, which is also a carbonate rock, has very different weathering characteristics and capacity than limestone. The rock weathering fissures were dense and narrow, and the soil was shallow (<20 cm) and suitable for herbaceous plants but had difficulty supporting the growth of trees. However, the soil of the dolomite slope was mostly fine herbaceous plant roots, and although it could effectively reduce the soil bulk density, the herbaceous roots were still weaker than the noncapillary pore space for the formation of gravity water channels for vegetation types of trees or scrub (Liu et al., 2019; Zhu et al., 2020). The weathering of limestone forms large, deep fissures along which surface soil is washed into the ground, causing soil erosion while exposing bedrock. It has been noted that the soil that fills the deep fissures in karst slopes due to soil erosion is rich in water that is difficult to evaporate, which could provide more available water for deep–rooted plants (Rong et al., 2011). Furthermore, the soil–rock structure of bedrock outcrops plays an important role in the distribution of water and organic carbon at the local scale (Wang et al., 2019b). Scholars believed that rock surface splash and interception caused by outcrop bedrock could increase the SOC and nutrient inputs to the soil and that when the rock to soil patch ratio was 7:3 or higher, the contribution of exposed rock to water and nutrient distribution could outweigh the effect of atmospheric deposition (Zhang et al., 2016).

Therefore, although the limestone slopes with exposed bedrock could provide limited water for plant growth and development, the exposed bedrock promoted the pooling of soil water and nutrients with limited storage capacity so that it could support the growth and development of vegetation such as trees and shrubs, while the dolomite slopes with different lithologies had more noncapillary pore spaces with shallow soil texture, which could provide more available water sources for plant growth and development (Table 4). However, these were limited by the impact of shallow soil layers, causing rapid evaporation and water leakage, which made it difficult to support similar limestone slopes for trees or shrubs, mainly herbaceous species.

4.2. *Effects of land-use change on soil hydrological characteristics*

In the karst region of Southwest China, in addition to the soil types and soil–rock structures discussed above, which had an impact on the hydrological characteristics of soils in the region, unreasonable human activities in the past have led to soil erosion resulting in rock desertification, and after years of environmental management projects, the soils in the region were bound to be affected accordingly. In this study, LS was used as a grazing slope in the past, and a study showed that its soil erosion was up to 69.31 Mg $km^{-2}year^{-1}$. The reason for this was that this kind of slope with grass mosaic shrubs was influenced by overgrazing and frequent trampling of the land between scrubs, which led to soil consolidation and a higher capacity, which affected the hydrological process of the slope surface and thus led to soil erosion (Peng and Wang, 2012). After ten years of natural vegetation restoration by grazing bans, the soil of karst slopes (LS) used for grazing still had a high soil bulk density (1.19 ~ 1.26 g·cm^{-3}), which indicates that the soil that was compacted in the past had not been effectively improved because the shallow soil on karst slopes is in direct contact with the underlying bedrock when trampled by livestock, and thus, there is a high compaction intensity. This type of soil compaction caused by such external disturbance may persist for decades, and the influencing factors include vegetation, soil type, topography, and climatic conditions (Rogger et al., 2017). Furthermore, soil erosion caused by overgrazing in the past changed the soil texture, resulting in an extremely high sand content (0.05 ~ 2 mm) and coarse–grained soil, which significantly contributed to the soil infiltration capacity (Table 2). The change in soil texture, while altering infiltration, also affected the ability to supply water to plants, and the increase in sand content at the LS sample site after the occurrence of severe erosion reduced the available water content. Human activities on agricultural land had a clear impact on the soil. It has been demonstrated that the soil surface layer of annually tilled agricultural land has a higher infiltration capacity, which is attributed to the mixing and homogenizing effect of agricultural land annual tilling activities, which increase the proportion of large pores conducive to water transport (Lipiec et al., 2006). This also explained why the yellow limestone soil (YLT) at the foot of the slope, which was cultivated year–round, had a higher infiltration capacity than the slope (LS) in this study, while the yellow soil sample with peach trees was not tilled, resulting in the surface layer K_s being only one–third of that of the

Table 5
Correlation analysis of soil properties with K_S and AWC.

	pH	BD	SOC	CP	NCP	Sand	Silt	Clay
FC	−0.171	−0.279	−0.001	−0.282	−0.092	0.031	0.338	−0.409
PWP	−0.068	0.269	−0.248	−0.426	0.105	0.494	−0.249	−0.427
AWC	−0.083	−0.560*	0.276	0.819**	−0.228	−0.544*	0.678**	0.034
K_s	0.247	0.299	0.339	−0.522*	0.442	0.728**	−0.723**	−0.247

DG means dolomite slope grassland; LS means limestone slope shrub; LA means limestone slope abandoned farmland; YLT means yellow limestone soil tillage; YFT means yellow soil tillage fruit forest; YF means yellow soil forestland; BD means soil bulk density; SOC means soil organic carbon; CP means soil capillary porosity; NCP means soil noncapillary porosity; Sand means soil sand content; Silt means soil silt content; Clay means soil clay content; pH means soil pH. * Correlation is significant at the 0.05 level, ** Correlation is significant at the 0.01 level.

YF sample, which was also yellow soil. However, the impact of human farming activities also had a significant effect on the organic carbon content, while affecting the water transport capacity of the soil and resulting in low organic carbon content (Chen et al., 2007).

4.3. Available water storage capacity per unit area of soil under the influence of soil–rock structures on karst slopes

Soil available water content is influenced by soil properties and human activities, and the complex soil–rock structures of carbonate rocks also play a role in the ability of vegetation to get water from the soil. In this study, the research result that the bedrock exposure rate in severe karst rocky desertification areas could be as high as 85% in the classification of rock desertification grade by Wang et al. (2004) was referenced. It was assumed that the percentage of slope soil in the karst area per unit area was 15 ~ 100%, and Table 6 was derived according to the soil available water content in the previous paper. It is clear from the table that the soil available water content for plant uptake per unit area on limestone slopes was significantly reduced due to the exposed bedrock, indicating that it is difficult to provide more available water sources for vegetation per unit area on karst slopes. From the rock fractures in the semiweathered layer beneath the shallow soil, this proportion could reach more than 90% and up to 100% in the dry season (Rong et al., 2011). The dolomite intercrystalline voids were uniform, which facilitated the overall dissolution effect and made it difficult to produce larger fissures, so the dolomite slope soil was relatively uniform and shallowly distributed on the surface, and there were many gravels (Rong et al., 2011; Liu et al., 2019). In conclusion, the exposed bedrock of the dolomite slope compressed and reduced soil water storage. Large trees found it difficult to survive quick hydrological processes due to shallow strata and semiregolith (Rong et al., 2011; Liu et al., 2019).

In summary, the soil hydrological characteristics in karst areas are influenced by various aspects of soil texture, soil–rock structures, and land use. Among them, the available water supply was dependent on soil properties, especially soil texture. The soil properties in the karst area were influenced by soil types and land use, in addition to being controlled by the soil–rock structures caused by the special geological background of this area. The increase in the proportion of rock outcrops per unit area of land inevitably compressed the total amount of soil, thus controlling the actual available water supply capacity, which eventually manifested itself as the difference between vegetation type and land use (Fig. 4) (Rong et al., 2011; Zhang et al., 2012; Chen et al., 2022). According to related studies, the low total soil amount in the karst areas of Southwest China results in low forest productivity and biomass, which are far lower than those of tropical low–mountain evergreen broad–leaved forests and artificial forests with similar hydrothermal conditions and far lower than those of high–latitude coniferous and broad–leaved mixed forests and alpine coniferous forests with similar hydrothermal conditions (Liu et al., 2009; Guo et al., 2011; Liu et al., 2019).

Table 6
Soil actual available water content per unit area (mm).

Depth (cm)	DG	LS	LA	YLT	YFT	YF
0 ~ 10	6.49 ~ 43.26	2.66 ~ 17.73	5.21 ~ 34.72	29.87	27.30	20.16
10 ~ 20		3.51 ~ 23.39	3.46 ~ 23.04	20.95	27.23	30.51
20 ~ 30		3.46 ~ 23.06	3.40 ~ 22.64	23.41	35.25	24.16

The DG, LS and LA sample lands were carbonate slope lands with shallow soil layers and various degrees of exposed bedrock. According to the research results of Wang (2004), the rocky desertification rate can exceed 85%, so we multiplied the soil available water of the carbonate slope lands in Table 3 by 15% to obtain the values shown in Table 5.

We believe that the difference in bedrock exposure per unit area of land in karst environments and vegetation growth are inextricably linked. Only grass and a few drought–tolerant shrubs thrived on the dolomite slope, as shown in Fig. 4 (a), since the soil storage capacity is shallow and accompanied by bare bedrock, and the soil storage space is constrained both vertically and horizontally. In contrast, on limestone slopes (b) and (c), the different extents of exposed bedrock led to a different degree of slope soil storage space compression, which controlled the growth of vegetation and soil water storage, and as a result of the junction between rock and soil macropores accelerating the speed of water infiltration, the growth and development of large trees were further limited. Finally, Fig. 4 (d) depicts yellow limestone soil and yellow soil with deep soil layers, both of which are favorable for vegetation growth and development. As a result, agricultural operations or the planting of tall trees are common in yellow limestone soil and yellow soil places.

4.4. Relationship between water availability and land use of vegetation on karst slopes

On nonkarstic slopes, soil properties and water-holding characteristics are the key factors determining land use and agricultural development; however, on karstic slopes, there is also the influence of the complex geological background (Fu et al., 2000; Kang et al., 2002; Katuwal et al., 2020). On the dolomite slopes, the soil thickness hardly exceeded 30 cm, but there were some fissures filled with soil on dolomite slopes. Such a kind of fissured soil similar to limestone slopes could provide a reliable space for vegetation growth. Yang et al. (2016) studied the hydrological characteristics of soil-filled fissures in three typical fissures after the excavation of dolomite slopes and found that all fissure fillings had excellent water retention capacity and could provide a reliable water source for vegetation survival. However, the dolomite slope per unit area is limited by the double influence of shallow soil and bare bedrock, and the total amount of soil rarely increases the space from which vegetation can obtain water, which is also the reason why the vegetation growth of dolomite slopes under natural restoration is inferior to that of limestone slopes (Fig. 5) (Liu et al., 2019).

For limestone slopes, unreasonable land use has caused strong soil erosion, land quality decline, and rock desertification with exposed bedrock in the past, and the vegetation has been restored after years of ecological management (Peng and Wang, 2012; Jiang et al., 2014). According to the actual soil available water content per unit area of limestone slopes, we envisioned in the previous article, under the geomorphic structure of interlocking rock and soil distribution, the total amount of soil was low due to its fragmented distribution, which eventually led to the shortage of soil available water per unit area for vegetation growth (Table 5). Although the total amount of soil per unit area was reduced on limestone slopes to support the growth of trees, the exposed carbonate rocks also had a pooling effect on water, and the rock–soil interface allowed precipitation to enter the small amount of soil more quickly to achieve vegetation growth and development (Sohrt et al., 2014; Liu et al., 2016). This process was fundamentally different from the lack of rainfall in semiarid areas that damages soil properties and thus limits vegetation development. The lack of water recharge in semiarid areas where the deep layer of vegetation absorbs water and cannot be recharged in time will produce a soil drying layer, which can be regulated by increasing in situ infiltration and reducing vegetation evapotranspiration (Shao et al., 2016). The karst region in Southwest China has abundant rainfall and good vegetation cover, but the water infiltration rate is too fast due to the rock–soil interface and underground pore space. It is difficult for the shallow soil to maintain water, and the suitable vegetation is mostly drought–tolerant and calcium–loving species (Sohrt et al., 2014; Liu et al., 2019). The yellow soil distributed in the peak–forest plain and peak–cluster vallery is a typical soil type in southern China. In this study, the available water of the yellow soil was higher than that of the nonzoned sloping limestone soil,

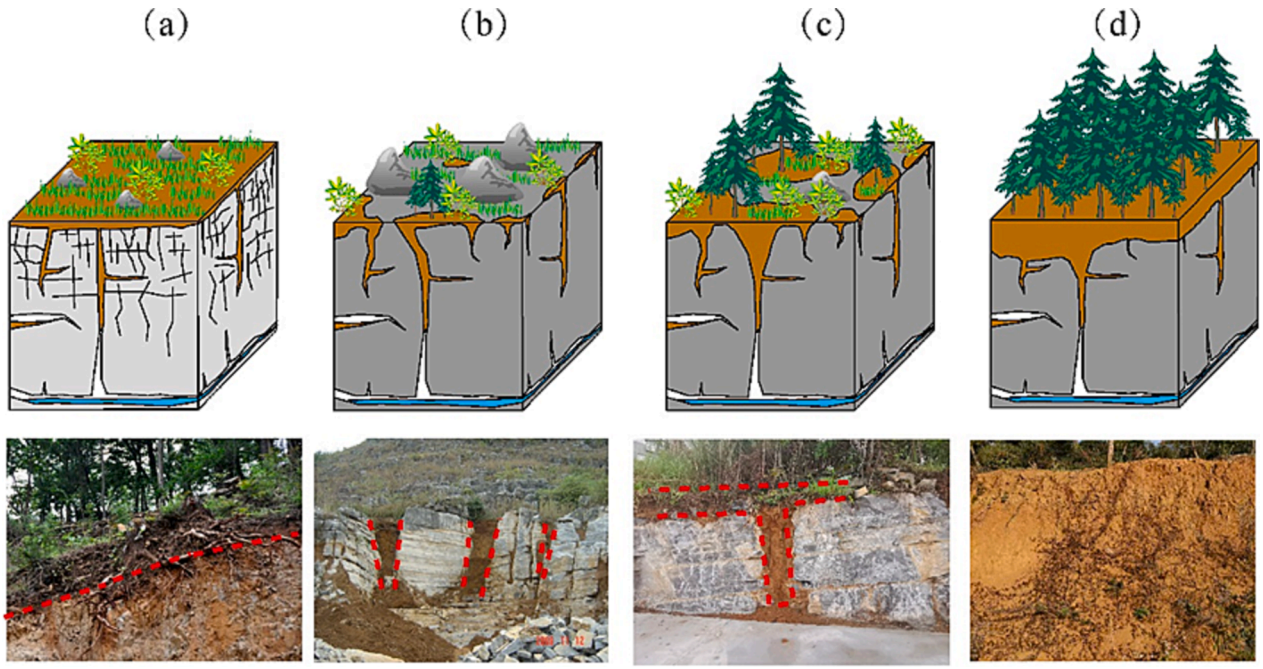

Fig. 4. Change in rock and soil structure. (a) Dolomite geotechnical structure; (b) more rock exposure limestone slope; (c) less exposed rock limestone slope; (d) no rock exposure (yellow soil or yellow limestone soil).

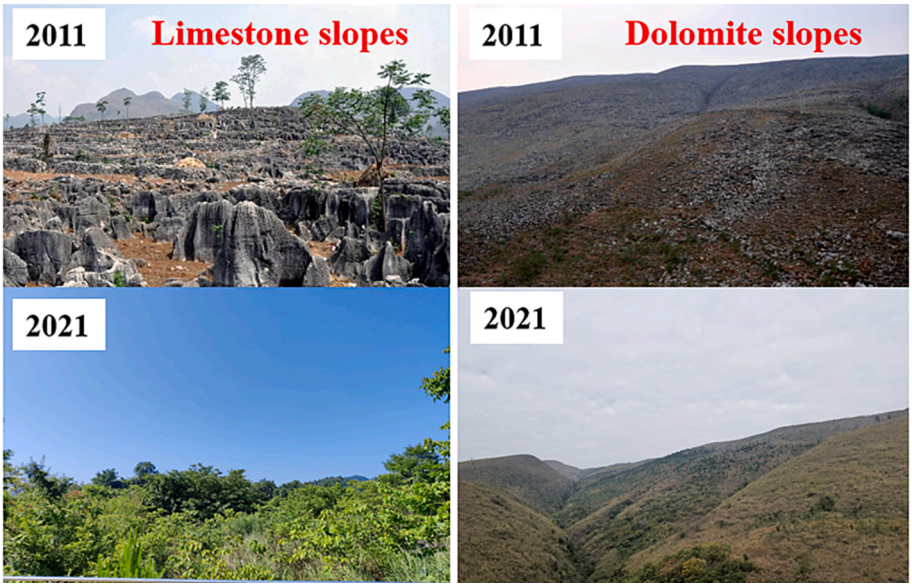

Fig. 5. Multiyear restoration of vegetation on carbonate slopes of different lithologies.

which can provide more water for vegetation, and its distribution area was mostly on gentle slopes and plains. Moreover, the soil layer was deep, usually planted with *P. massoniana*, tea trees and other acid–loving soil species to increase the income of the economy. To pursue the economic effect, the soil acidification caused by the excessive use of chemical fertilizers and the soil erosion and soil pollution in the peak–forest plain and peak–cluster vallery areas where human activities are frequent need reasonable use and treatment (Li et al., 2012; Yan et al., 2018).

In summary, the limestone soil formed by the weathering of carbonate rocks due to the different lithology of its parent rock caused by the difference in vegetation growth between limestone slopes and dolomite slopes can be seen. Karst slopes should be based on the difference in lithology to determine the production of water, and dolomite slopes with shallow soil and exposed bedrock should consider shallow root systems with less water consumption of scrub vegetation for restoration. Limestone slopes can use local fissure soil to develop local characteristics of warped fruit forest (prickly pear, plum, etc.). Additionally, to solve the problems of rapid hydrological processes and weak soil water content of karst slopes, relevant small reservoirs should be supported. Luckily, researchers have noted that the development of effective rainwater utilization technologies for roads, roofs and surfaces, in situ rainfall storage and related cisterns can effectively solve the problem of water shortage under abundant rainfall in karst areas (Zhang et al., 2012; Qin et al., 2015).

5. Conclusion

Based on the analysis of the soil hydraulic characteristics of a typical watershed in a karst area, the effects of multiple factors on the water transport capacity of typical soils and the soil available water supply capacity were discussed. The study showed that the differences in basic soil properties between the zonally distributed yellow soil and the nonzonally distributed limestone soil due to different soil types were caused by the heterogeneity of the hydrological characteristics of karst soil. The impact of human activities on the hydrological function of soil in karst is long-term, and the soil water supply and transport capacity of carbonate slopes severely damaged by humans remain poor after a decade of natural restoration. The difference in soil–rock structures controls the soil hydrological characteristics in karst areas. The bare bedrock of carbonate slopes reduces the total amount of soil per unit area, compresses the total amount of soil available water storage per unit area for plant growth, and inhibits plant growth. In contrast, the difference in the soil–rock structure produced by the different lithologies of limestone and dolomite controls the distribution of vegetation types on slopes. The soil resources of carbonate slopes are valuable and difficult to recover after being damaged by strong human activities, which should continue to be prohibited. The factors affecting soil hydrological characteristics in karst areas are complex, and the weights of each factor on soil hydrological characteristics will be deepened and refined in future research. The weights of the influence of soil type, lithology, and soil–rock structures should be considered in future related soil water use.

Declaration of Competing Interest

The authors declare that they have no known competing financial interests or personal relationships that could have appeared to influence the work reported in this paper.

Data availability

The data that has been used is confidential.

Acknowledgements

The work described in this paper was supported by the Strategic leading science and technology project of Chinese Academy of Sciences (XDB40020201), National Natural Science Foundation of China (42261144672, 42230509, 42077317), Key Project of Basic Research of Guizhou Provincial Department of Science and Technology ([2022] 048, GZ2020SIG), Science and Technology Service Network Initiative of Chinese Academy Sciences (KFJ-STS-QYZD-2021-24-001). The authors would like to express their gratitude to the editor and anonymous reviewers for their valuable comments and suggestions.

References

Bagarello, V., D'Asaro, F., Iovino, M., 2012. A field assessment of the Simplified Falling Head technique to measure the saturated soil hydraulic conductivity. Geoderma 187, 49–58. https://doi.org/10.1016/j.geoderma.2012.04.008.

Bai, Y.X., Zhou, Y.C., 2020. The main factors controlling spatial variability of soil organic carbon in a small karst watershed, Guizhou Province, China. Geoderma 357, 113938. https://doi.org/10.1016/j.geoderma.2019.113938.

Cao, J.H., Yuan, D.X., Pan, G.X., 2003. Some soil features in karst ecosystem (in Chinese). Adv. Earth Sci. 18, 37–44. https://doi.org/10.3321/j.issn:1001-8166.2003.01.006.

Cao, J.H., Jiang, Z.C., Yang, D.S., Pei, J.G., Yang, H., Luo, W.Q., 2008. Grading of soil erosion intensity in Southwest karst area of China. Sci. Soil Water Conser. 6, 1–7. https://doi.org/10.16843/j.sswc.2008.06.001.

Cardelli, V., Cocco, S., Agnelli, A., Nardi, S., Pizzeghello, D., Fernandez-Sanjurjo, M.J., Corti, G., 2017. Chemical and biochemical properties of soils developed from different lithologies in Northwestern Spain (Galicia). Forests 8, 135. https://doi.org/10.3390/f8040135.

Chen, L., Gong, J., Fu, B.J., Huang, Z., Huang, Y., Gui, L., 2007. Effect of land use conversion on soil organic carbon sequestration in the loess hilly area, loess plateau of China. Ecol. Res. 22, 641–648. https://doi.org/10.1007/s11284-006-0065-1.

Chen, H., Liu, J., Zhang, W., Wang, K., 2012. Soil hydraulic properties on the steep karst hillslopes in northwest Guangxi, China. Environ. Earth Sci. 66, 371–379. https://doi.org/10.1007/s12665-011-1246-y.

Chen, J., Luo, W., Zeng, G., Wang, Y., Lyu, Y., Cai, X., Zhang, L., Cheng, A., Zhang, X., Wang, S., 2022. Response of surface evaporation and subsurface leakage to precipitation for simulated epikarst with different rock-soil structures. J. Hydrol. 610, 127850 https://doi.org/10.1016/j.jhydrol.2022.127850.

Chen, X., Zhang, Z., Chen, X., Shi, P., 2009. The impact of land use and land cover changes on soil moisture and hydraulic conductivity along the karst hillslopes of southwest China. Environ. Earth Sci. 59, 811–820. https://doi.org/10.1007/s12665-009-0077-6.

Davey, B.G., Russell, J.D., Wilson, M.J., 1975. Iron-oxide and clay-minerals and their relation to colours of red and yellow podzolic soils near Sydney, Australia. Geoderma 14, 125–138. https://doi.org/10.1016/0016-7061(75)90071-3.

Di, X., Xiao, B., Dong, H., Wang, S., 2019. Implication of different humic acid fractions in soils under karst rocky desertification. Catena 174, 308–315. https://doi.org/10.1016/j.catena.2018.11.028.

Ford, D., Williams, P.D., 2007. Karst hydrogeology and geomorphology. Wiley, Chichester, West Sussex, England.

Fu, B.J., Chen, L.D., Ma, K.M., Zhou, H.F., Wang, J., 2000. The relationships between land use and soil conditions in the hilly area of the loess plateau in northern Shaanxi, China. Catena 39, 69–78. https://doi.org/10.1016/s0341-8162(99)00084-3.

Fu, Z.Y., Chen, H.S., Zhang, W., Xu, Q.X., Wang, S., Wang, K.L., 2015. Subsurface flow in a soil-mantled subtropical dolomite karst slope: A field rainfall simulation study. Geomorphology 250, 1–14. https://doi.org/10.1016/j.geomorph.2015.08.012.

Fu, T., Chen, H., Fu, Z., Wang, K., 2016. Surface soil water content and its controlling factors in a small karst catchment. Environ. Earth Sci. 75, 1–11. https://doi.org/10.1007/s12665-016-6222-0.

Guo, K., Liu, C.C., Dong, M., 2011. Ecological adaptation of plants and control of rocky-desertification on karst region of South-west China (in Chinese). J. Plant Ecol. 35, 991–999. https://doi.org/10.3724/SP.J.1258.2011.00991.

Han, C., Song, M., Du, H., Zeng, F., Peng, W., Wang, H., Chen, L., Su, L., 2017. Biomass and carbon storage in roots of *Cunninghamia lanceolata* and *Pinus massoniana* plantations at different stand ages in Guangxi (in Chinese). Acta Ecol. Sin. 37, 2282–2289. https://doi.org/10.5846/stxb201511292394.

Jiang, Z., Lian, Y., Qin, X., 2014. Rocky desertification in Southwest China: Impacts, causes, and restoration. Earth Sci. Rev. 132, 1–12. https://doi.org/10.1016/j.earscirev.2014.01.005.

Jonsson, M., Dimitriou, I., Aronsson, P., Elowson, T., 2004. Effects of soil type, irrigation volume and plant species on treatment of log yard run-off in lysimeters. Water Res. 38, 3634–3642. https://doi.org/10.1016/j.watres.2004.05.017.

Kang, S.Z., Zhang, L., Liang, Y.L., Hu, X.T., Cai, H.J., Gu, B.J., 2002. Effects of limited irrigation on yield and water use efficiency of winter wheat in the Loess Plateau of China. Agric. Water Manag. 55, 203–216. https://doi.org/10.1016/s0378-3774(01)00180-9.

Katuwal, K.B., Cho, Y., Singh, S., Angadi, S.V., Begna, S., Stamm, M., 2020. Soil water extraction pattern and water use efficiency of spring canola under growth-stage-based irrigation management. Agric. Water Manag. 239, 106232 https://doi.org/10.1016/j.agwat.2020.106232.

Kramer, P.J., 1969. Plant and soil water relationships: A modern synthesis. McGraw-Hill, New York.

Li, H., Ma, Y., Liu, W., Liu, W., 2012. Soil changes induced by rubber and tea plantation establishment: comparison with tropical rain forest soil in Xishuangbanna, SW China. Environ. Manag. 50, 837–848. https://doi.org/10.1007/s00267-012-9942-2.

Lipiec, J., Kus, J., Slowinska-Jurkiewicz, A., Nosalewicz, A., 2006. Soil porosity and water infiltration as influenced by tillage methods. Soil Till. Res. 89, 210–220. https://doi.org/10.1016/j.still.2005.07.012.

Liu, C.C., Wei, Y.F., Liu, Y.Q. and Guo, K., 2009. Biomass of canopy and shrub layers of Karst forests in Puding, Guizhou, China (in Chinese). J. Plant Ecol. 33. https://doi.org/CNKI:SUN:ZWSB.0.2009-04-010.

Liu, H., Jiang, Z., Dai, J., Wu, X., Peng, J., Wang, H., Meersmans, J., Green, S.M., Quine, T.A., 2019. Rock crevices determine woody and herbaceous plant cover in the karst critical zone. Sci. China Earth Sci. 62, 1756–1763. https://doi.org/10.1007/s11430-018-9328-3.

Liu, C., Liu, Y., Guo, K., Wang, S., Liu, H., Zhao, H., Qiao, X., Hou, D., Li, S., 2016. Aboveground carbon stock, allocation and sequestration potential during vegetation recovery in the karst region of southwestern China: A case study at a watershed scale. Agr. Ecosyst. Environ. 235, 91–100. https://doi.org/10.1016/j.agee.2016.10.003.

Liu, S., Wang, Y., An, Z., Sun, H., Zhang, P., Zhao, Y., Zhou, Z., Xu, L., Zhou, J., Qi, L., 2021. Watershed spatial heterogeneity of soil saturated hydraulic conductivity as affected by landscape unit in the critical zone. Catena 203, 105322.

Mujica, C.R., Bea, S.A., 2020. Estimations of rooting depths and sources of plant-available water (PAW) in flatland petrocalcic soils under different land uses. Geoderma 361, 114019.

Ni, J., Luo, D.H., Xia, J., Zhang, Z.H., Hu, G., 2015. Vegetation in karst terrain of southwestern China allocates more biomass to roots. Solid Earth 6, 799–810. https://doi.org/10.5194/se-6-799-2015.

Nie, Y., Chen, H., Wang, K., Ding, Y., 2014. Rooting characteristics of two widely distributed woody plant species growing in different karst habitats of southwest China. Plant Ecol. 215, 1099–1109. https://doi.org/10.1007/s11258-014-0369-0.

Ouyang, Y., 2002. Phytoremediation: modeling plant uptake and contaminant transport in the soil-plant-atmosphere continuum. J. Hydrol. 266, 66–82. https://doi.org/10.1016/s0022-1694(02)00116-6.

Peng, X., Dai, Q., Ding, G., Li, C., 2019a. Role of underground leakage in soil, water and nutrient loss from a rock-mantled slope in the karst rocky desertification area. J. Hydrol. 578, 124086.
Peng, X., Dai, Q., Ding, G., Shi, D., Li, C., 2019b. The role of soil water retention functions of near-surface fissures with different vegetation types in a rocky desertification area. Plant Soil 441, 587–599. https://doi.org/10.1007/s11104-019-04147-1.
Peng, T., Wang, S., 2012. Effects of land use, land cover and rainfall regimes on the surface runoff and soil loss on karst slopes in southwest China. Catena 90, 53–62. https://doi.org/10.1016/j.catena.2011.11.001.
Qin, L., Bai, X., Wang, S., Zhou, D., Li, Y., Peng, T., Tian, Y., Luo, G., 2015. Major problems and solutions on surface water resource utilisation in karst mountainous areas. Agric. Water Manag. 159, 55–65. https://doi.org/10.1016/j.agwat.2015.05.024.
Reynolds, W.D., Bowman, B.T., Brunke, R.R., Drury, C.F., Tan, C.S., 2000. Comparison of tension infiltrometer, pressure infiltrometer, and soil core estimates of saturated hydraulic conductivity. Soil Sci. Soc. Am. J. 64, 478–484. https://doi.org/10.2136/sssaj2000.642478x.
Reynolds, W.D., Elrick, D.E., 1990. Ponded infiltration from a single ring: I. Analysis of steady flow. Soil Sci. Soc. Am. J. 54, 1233–1241. https://doi.org/10.2136/sssaj1990.03615995005400050006x.
Rogger, M., Agnoletti, M., Alaoui, A., Bathurst, J.C., Bodner, G., Borga, M., Chaplot, V., Gallart, F., Glatzel, G., Hall, J., Holden, J., Holko, L., Horn, R., Kiss, A., Kohnova, S., Leitinger, G., Lennartz, B., Parajka, J., Perdigao, R., Peth, S., Plavcova, L., Quinton, J.N., Robinson, M., Salinas, J.L., Santoro, A., Szolgay, J., Tron, S., van den Akker, J.J.H., Viglione, A., Bloeschl, G., 2017. Land use change impacts on floods at the catchment scale: Challenges and opportunities for future research. Water Resour. Res. 53, 5209–5219. https://doi.org/10.1002/2017wr020723.
Rong, L., Chen, X., Chen, X., Wang, S., Du, X., 2011. Isotopic analysis of water sources of mountainous plant uptake in a karst plateau of southwest China. Hydrol. Process. 25, 3666–3675. https://doi.org/10.1002/hyp.8093.
Salter, P.J., Williams, J.B., 1965. The influence of texture on the moisture characteristics of soils. II. Available water capacity and moisture release characteristics. J. Soil Sci. 16, 310. https://doi.org/10.1111/j.1365-2389.1965.tb01442.x.
Schelle, H., Iden, S.C., Peters, A., Durner, W., 2010. Analysis of the agreement of soil hydraulic properties obtained from multistep-outflow and evaporation methods. Vadose Zone J. 9, 1080–1091. https://doi.org/10.2136/vzj2010.0050.
Schelle, H., Heise, L., Jaenicke, K., Durner, W., 2013. Water retention characteristics of soils over the whole moisture range: a comparison of laboratory methods. Eur. J. Soil Sci. 64, 814–821. https://doi.org/10.1111/ejss.12108.
Shao, M.a., Jia, X., Wang, Y. and Zhu, Y., 2016. A review of studies on dried soil layers in the Loess Plateau (in Chinese). Adv. Earth Sci. 31, 14-22. https://doi.org/10.11867/j.issn.1001-8166.2016.01.0014.
Sohrt, J., Ries, F., Sauter, M., Lange, J., 2014. Significance of preferential flow at the rock soil interface in a semi-arid karst environment. Catena 123, 1–10. https://doi.org/10.1016/j.catena.2014.07.003.
Tong, X., Wang, K., Yue, Y. and Liao, C., 2013. Trends in vegetation change under different karst terrain conditions, southwest China. 8921, 393-398. https://doi.org/10.1117/12.2031737.
Wang, M., Chen, H., Zhang, W., Wang, K., 2018. Soil nutrients and stoichiometric ratios as affected by land use and lithology at county scale in a karst area, southwest China. Sci. Total Environ. 619, 1299–1307. https://doi.org/10.1016/j.scitotenv.2017.11.175.
Wang, J., Chen, X., Zhang, Z., Zhang, R., Zhu, B., Gong, Y., Liu, H., Yuan, S., 2019a. Preference flow at rock-soil interface and its influence on soil water dynamics in the karst troughs (in Chinese). Carsol. Sin. 38, 109–116. https://doi.org/10.11932/karst20190112.
Wang, S.J., Li, R.L., Sun, C.X., Zhang, D.F., Li, F.Q., Zhou, D.Q., Xiong, K.N., Zhou, Z.F., 2004. How types of carbonate rock assemblages constrain the distribution of karst rocky desertified land in Guizhou Province, PR China: Phenomena and mechanisms. Land Degrad. Dev. 15, 123–131. https://doi.org/10.1002/ldr.591.
Wang, Y., Shao, M., Han, X., Liu, Z., 2015. Spatial variability of soil parameters of the van genuchten model at a regional scale. Clean-Soil Air Water 43 (2), 271–278.
Wang, D., Shen, Y., Li, Y., Huang, J., Mao, J., 2016. Rock outcrops redistribute organic carbon and nutrients to nearby soil patches in three karst ecosystems in SW China. PLoS One 11 (8), e0160773.
Wang, K., Zhang, C., Chen, H., Yue, Y., Zhang, W., Zhang, M., Qi, X., Fu, Z., 2019b. Karst landscapes of China: patterns, ecosystem processes and services. Landsc. Ecol. 34, 2743–2763. https://doi.org/10.1007/s10980-019-00912-w.
Yan, P., Shen, C., Fan, L., Li, X., Zhang, L., Zhang, L., Han, W., 2018. Tea planting affects soil acidification and nitrogen and phosphorus distribution in soil. Agr. Ecosyst. Environ. 254, 20–25. https://doi.org/10.1016/j.agee.2017.11.015.
Yang, J., Nie, Y., Chen, H., Wang, S., Wang, K., 2016. Hydraulic properties of karst fractures filled with soils and regolith materials: Implication for their ecohydrological functions. Geoderma 276, 93–101. https://doi.org/10.1016/j.geoderma.2016.04.024.
Yang, J., Xu, X., Liu, M., Xu, C., Zhang, Y., Luo, W., Zhang, R., Li, X., Kiely, G., Wang, K., 2017. Effects of "Grain for Green" program on soil hydrologic functions in karst landscapes, southwestern China. Agr. Ecosyst. Environ. 247, 120–129. https://doi.org/10.1016/j.agee.2017.06.025.
Zhang, Z., Huang, X., Zhou, Y., 2021. Factors influencing the evolution of human-driven rocky desertification in karst areas. Land Degrad. Dev. 32, 817–829. https://doi.org/10.1002/ldr.3731.
Zhang, W., Liu, C., Wang, Z., Zhang, L., Luo, X., 2014. Speciation and isotopic composition of sulfur in limestone soil and yellow soil in karst areas of Southwest China: implications of different responses to acid deposition. J. Environ. Qual. 43, 809–819. https://doi.org/10.2134/jeq2013.09.0359.
Zhang, X., Wang, S., Meng, T., 2012. Rocky desertification sloping farmland management model. Soil Water Conserv. China 4. https://doi.org/10.3969/j.issn.1000-0941.2012.09.018.
Zhang, M., Wang, K., Liu, H., Wang, J., Zhang, C., Yue, Y., Qi, X., 2016. Spatio-temporal variation and impact factors for vegetation carbon sequestration and oxygen production based on rocky desertification control in the karst region of Southwest China. Remote Sens. (Basel) 8, 102. https://doi.org/10.3390/rs8020102.
Zhao, X., Wu, P., Gao, X., Tian, L., Li, H., 2014. Changes of soil hydraulic properties under early-stage natural vegetation recovering on the Loess Plateau of China. Catena 113, 386–391. https://doi.org/10.1016/j.catena.2013.08.023.
Zhong, F., Xu, X., Li, Z., Zeng, X., Yi, R., Luo, W., Zhang, Y., Xu, C., 2022. Relationships between lithology, topography, soil, and vegetation, and their implications for karst vegetation restoration. Catena 209, 105831. https://doi.org/10.1016/j.catena.2021.105831.
Zhu, T., Zeng, S., Qin, H., Zhou, K., Yang, H., Lan, F., Huang, F., Cao, J., Mueller, C., 2016. Low nitrate retention capacity in calcareous soil under woodland in the karst region of southwestern China. Soil Biol. Biochem. 97, 99–101. https://doi.org/10.1016/j.soilbio.2016.03.001.
Zhu, P., Zhang, G., Wang, H., Xing, S., 2020. Soil infiltration properties affected by typical plant communities on steep gully slopes on the Loess Plateau of China. J. Hydrol. 590, 125535 https://doi.org/10.1016/j.jhydrol.2020.125535.